

Implication of Absolute Calibration for Michelson Interferometer ECE Diagnostic at JET for ITER

S. Schmuck¹, J. Fessey², L. Figini³ and JET EFDA Contributors*

JET-EFDA, Culham Science Centre, Abingdon, OX14 3DB, UK

¹*Max-Planck-Institut für Plasmaphysik, Teilinstitut Greifswald, EURATOM-Assoziation,
D-17491 Greifswald, Germany*

²*Euratom/CCFE Fusion Association, Culham Science Centre, Abingdon, Oxon, OX14 3DB, UK*

³*Istituto di Fisica del Plasma, CNR, Euratom-ENEA-CNR Association, Milano, Italy*

1. Introduction

In the microwave and near infrared spectral range a Michelson interferometer diagnostic[1] is dedicated to probe the electron cyclotron emission (ECE) spectrum of several harmonics emitted by high-temperature plasmas in fusion experiments with magnetic confinement[2]. The standard analysis of the interferogram data reveals the electron temperature profile T_e . Besides the standard application a sophisticated technique can extract further information like about the electron density n_e , the equilibrium and wall properties[3]. However, the essential cornerstone for any analysis is the challenging absolute calibration of the diagnostic. Recently at JET, the calibration was carried out using the hot/cold technique with source temperatures well below 1000K ($\sim 0.0001\text{keV}$). The attempt demonstrates that the calibration factors can be determined with the relative uncertainty of $\sim 1.5\%$ in the spectral range 0.1-0.35THz[4,5]. With respect to the plasma parameters at JET the spectral range of interest is covered by the calibration. The situation changes for the ITER tokamak. For the envisaged plasma parameters $B=5.3\text{T}$, $T_e=25\text{keV}$ and $n_e=10^{20}\text{m}^{-3}$ the spectral range of interest lies beyond 0.5THz. Indeed the calibration and thus the T_e measurement are assured by probing the first harmonic in O-mode polarization[2,6], physics studies like for non-Maxwellian plasmas demand the calibration up to at least 1THz including spectral ranges for which the optical thickness is low. To accomplish the calibration on a reasonable time scale of some days the design of the ITER Michelson interferometer diagnostic is constraint by the required sensitivity, and design studies are on-going[7,8]. Nevertheless, the studies can be supported by implications of a well-characterized diagnostic like the JET interferometer and modelling the interferogram data giving constraints for the data acquisition system.

2. Michelson Interferometer Design for ITER

The minimum diagnostic sensitivity necessary to perform an absolute calibration up to 1THz during some days is estimated using measurements with the interferometer at JET. For the latter the relative

* See the Appendix of F. Romanelli et al., Proceedings of the 23rd IAEA FEC 2010, Daejeon, Korea

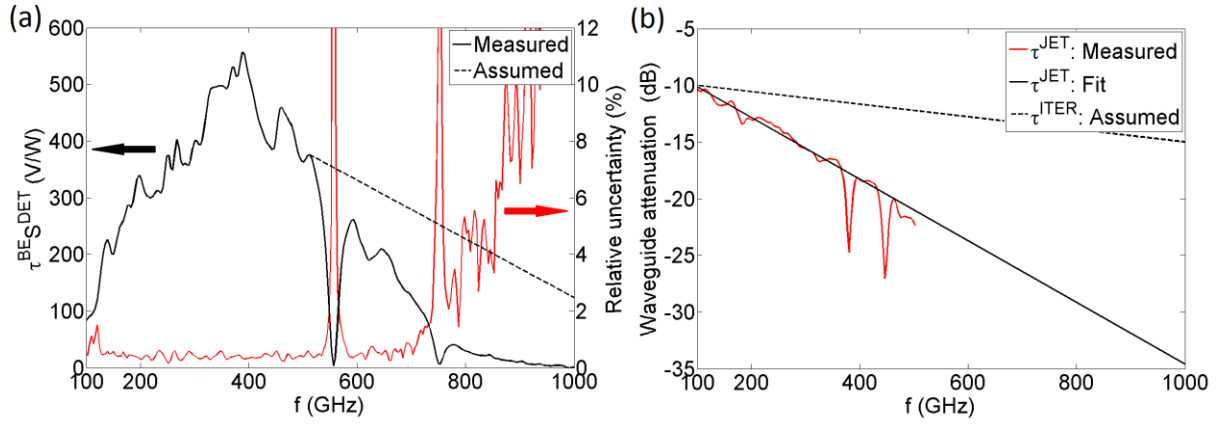


Figure 1: (a) Measured (black) and estimated (dashed) sensitivity of Michelson interferometer back end assuming an ideal antenna. (b) Measured (red) and estimated (dashed) attenuation of transmission lines.

uncertainty in the spectral domain, i.e. the inverse signal-to-noise ratio (SNR), is available. The relative uncertainty marks 0.5THz as the upper limit for the successful calibration of the interferometer at JET. Shifting the limit to 1THz for the diagnostic at ITER is achieved by a diagnostic design which increases the SNR as seen by the detector accordingly. The estimation of C^{ITER} uses the separation of the diagnostic into the general segments: antenna, transmission line and back end. The corresponding calibration factors dependent on frequency f can be written as $C^{ITER}(f) = (A_e \Omega_a) \tau^{ITER} (\tau_{BE}^{S^{DET}})$. Thereby, the product of the effective antenna area A_e and the antenna solid angle Ω_a characterizes the power collection by the antenna, the quantity τ^{ITER} expresses the power attenuation of the transmission line, and $\tau_{BE}^{S^{DET}}$ states the absolute sensitivity of the back end. Each segment is treated individually in the following.

An ideal antenna is assumed for which the power coupling into the waveguide is given by $A_e \Omega_a = \lambda^2 = (c/f)^2$ [9]. The back end sensitivity $\tau_{BE}^{S^{DET}}$ of the JET interferometer is shown Fig. 1a assuming an ideal antenna. By replacing/removing the infra-red filter used in the JET diagnostic $\tau_{BE}^{S^{DET}}$ should be improved. Assuming this action transfers the set point 120V/W to 1THz, a falling ramp for $\tau_{BE}^{S^{DET}}$ is used above 0.5THz for modelling (see Fig. 1a). The attenuation τ^{JET} of the JET transmission line follows from the ratio of the absolute calibration factors derived for placing the hot- and cold-source in front of the in-lab and in-vessel antenna, respectively. Thereby, the relative uncertainty for the in-vessel set becomes large above 0.5THz restricting the derivation (see Fig. 2a). On logarithmic scale τ^{JET} falls almost linearly (-10 to -21dB) for the spectral range 0.1-0.5THz (see Fig. 1b). To transfer the relative uncertainty from 0.5THz to 1THz the power leaving each waveguide needs to be the same. Therefore, since the power coupling of the antenna is assumed to decay with f^{-2} , the attenuation τ^{ITER} has to compensate the factor 4. Thus, τ^{ITER} must exceed -15dB at 1THz. For the modelling purpose τ^{ITER} is chosen to decrease linearly from -10dB to -15dB on logarithmic scale (see Fig. 1b). The minimum sensitivity C^{ITER} (see Fig. 3a) of the Michelson interferometer for ITER necessary to achieve an absolute calibration up to 1THz during some days of integration time using sources with temperatures below 1000K is estimated assuming

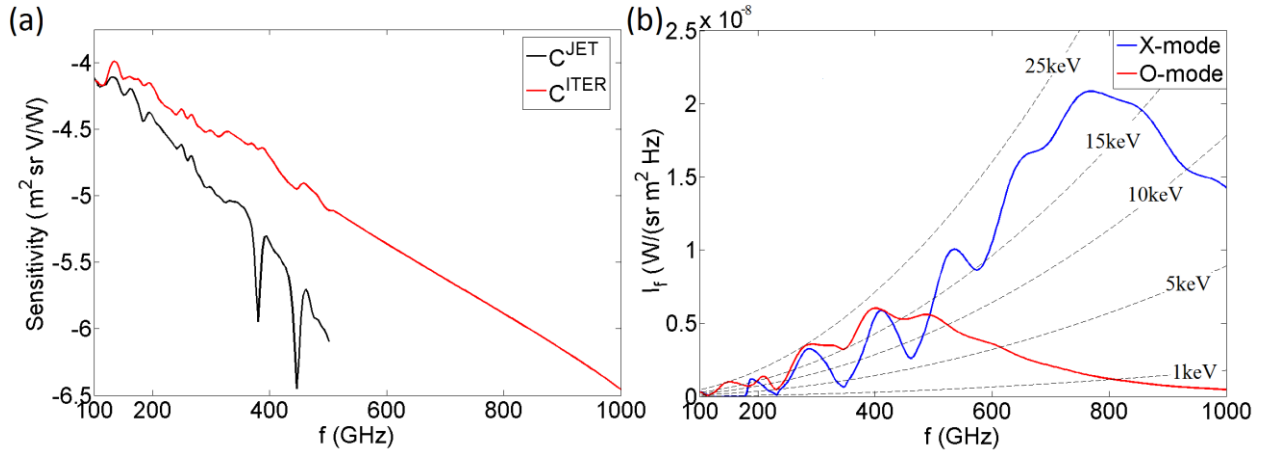


Figure 2: (a) Measured sensitivity C^{JET} (black) and estimated minimum sensitivity C^{ITER} (red) required for calibration up to 1THz. (b) Predicted ECE spectrum I_f for pure O- and X-mode polarization for central $T_e=25\text{keV}$.

an ideal antenna, a water vapour free transmission line, using $\tau^{BE} S^{DET}$ from Fig. 1a and τ^{ITER} from Fig. 1b.

2.1. Predicted ECE Spectrum and Interferogram

The ECE ray-tracing code SPECE[10] predicts the ECE spectrum I_f for ITER conditions assuming inductive operation $I_p=15\text{MA}$, $P_H=400\text{MW}$, $B=5.3\text{T}$ at the magnetic axis, central $T_e=25\text{keV}$ and $n_e=10^{20}\text{m}^{-3}$, radial line of sight from low magnetic field side in the plasma equatorial plane. For pure O- and X-mode polarisation the predicted intensity spectrum available at the antenna aperture is shown in Fig. 2b for the spectral range 0.1-1THz with the spectral resolution $\Delta f=3.66\text{GHz}$. For the modelling each spectrum is presumed to vanish outside 0.1-1THz. For completeness, it is mentioned that the effect of mode scrambling due to wall reflections is omitted. By the diagnostic model $V(x) = \int I_f C^{ITER} \cos\left(2\pi \frac{f}{c} x\right) df$ the interferogram data V is predicted dependent on the optical path difference x . The ECE spectra in O- and X-mode polarization (see Fig. 2b) and the minimum sensitivity C^{ITER} derived (see Fig. 2a) enter as input quantities. The interferograms for each polarization is predicted for the optical path difference increment $\Delta x=5\mu\text{m}$ (see Fig. 3a). At the zero-path-difference (ZPD) position ($x=0$) the predicted detector output voltage exceeds 30mV. While the predicted interferogram can be evaluated on any spatial grid, the measured one is sampled with spatial period Δx and an offset x_0 with respect to the ZPD position. For X-mode polarization the interferograms to be measured are shown in Fig. 3b for $\Delta x=5, 20$ and $160\mu\text{m}$ and $x_0=0, 5$ and $40\mu\text{m}$, respectively. By eye the “continuous” interferogram represented by $\Delta x=5\mu\text{m}$ is sampled sufficiently for $\Delta x=20\mu\text{m}$. Clearly, for $\Delta x=160\mu\text{m}$ the sampling in the spatial domain becomes poor.

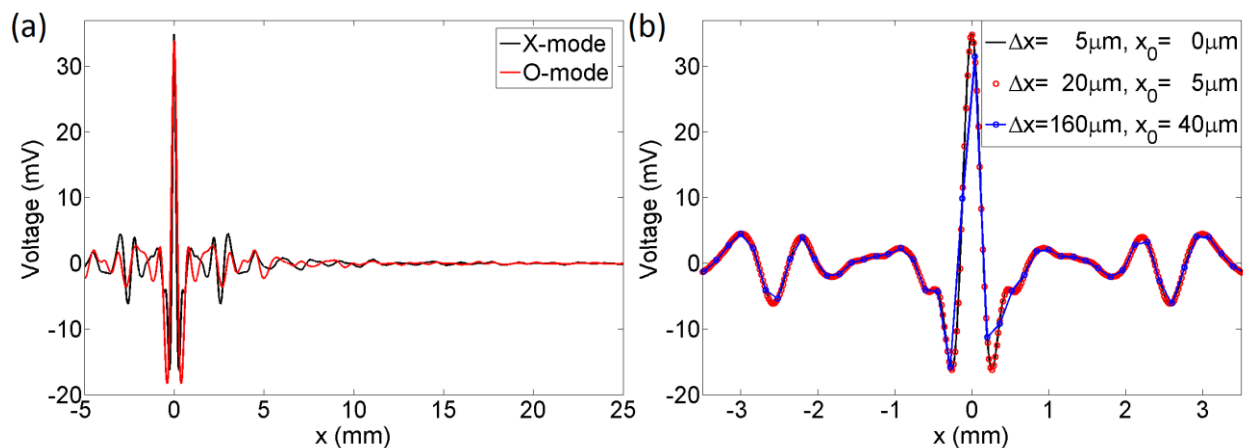


Figure 3: (a) Predicted interferogram for pure ECE spectrum in X- (black) and O-mode (red) polarization. (b) Effect of spatial sampling of interferogram around ZPD position for X-mode polarization.

2.2. Spectral Resolution, Sampling Frequency and DAQ System

Using fast Fourier transformation routines based on radix 2 the spectral resolution reads $\Delta f = c/(2^{k+1}\Delta x)$. Since $\Delta x = 20\mu\text{m}$ seems sufficient for spatial sampling (see Fig. 3b), the potential candidates for the ITER Michelson interferometer become $\Delta f = 1.83, 3.66$ and 7.32GHz for $k=12, 11$ and 10 , respectively. For the set $\Delta x = 20\mu\text{m}$, 3.66GHz and $\Delta t = 20\text{ms}$ the data acquisition (daq) system needs to cope with $f_s = 102.4\text{kHz}$ and even with $(\pi/2)f_s$ if the optical path difference is achieved by a moving mirror with sinusoidal acceleration like at JET.

3. Conclusions

To carry out an absolute calibration up to 1THz on a reasonable time of some days for the ITER Michelson interferometer its sensitivity was estimated. Thereby, the critical quantity is identified by the attenuation of the transmission line with the lower limit of -15dB at 1THz . This constraint is relaxed for an increased sensitivity of the interferometer back end. The prediction of the interferogram data using the estimated diagnostic sensitivity and a typical ECE spectrum for the spectral range $.1\text{-}1\text{THz}$ shows that the spatial sampling with increment $\Delta x = 20\mu\text{m}$ should be applied. As a consequence the daq system needs to cope with the sampling frequency of 200kHz assuming the spectral and temporal resolution 3.66GHz and 20ms , respectively.

Acknowledgement

This work was supported by EURATOM and carried out within the framework of the European Fusion Development Agreement Tasks. The views and opinions expressed herein do not necessarily reflect those of the European Commission.

References

- | | |
|---|--|
| [1] D.H. Martin and E. Puplett, <i>Infrared Phys.</i> 10, 105 (1969) | [3] S.Schmuck, 38 th EPS (2011) |
| [2] A.E. Costley., <i>Research. Fusion Sci. Technol.</i> , 55,1(2009) | [4] A.E. Costley, EC-3 (1982) |
| [5] S.Schmuck, To be submitted to <i>Rev. Sci. Instrum</i> (2012) | [6] S.Danani, <i>Fusion Sci. Technol.</i> 59, 4 (2011) |
| [7] H.K.Pandya, <i>Proc. of 17th EC</i> (2012) | [8] A.E. Costley, Private Communication (2012) |
| [9] J.D.Kraus, <i>Radio Astronomy</i> (1966) | [10] D. Farina, <i>AIP Conf. Proc.</i> 988, 128 (2008) |